Measured Attenuation and Depolarization of Light Transmitted Along Glass Fibers

By L. G. COHEN

(Manuscript received June 4, 1970)

Loss measurements have been made on glass fibers immersed in index matching oil. The measurements include state of polarization analyses of the light leaving fiber ends. The character of the beam was determined by using a $\lambda/4$ plate in conjunction with a polaroid analyser to measure the components of unpolarized and polarized light.

The data indicates that unclad fibers attenuate light much more than similar glass clad fiber waveguides. Mode purity within a multimode glass fiber was estimated from measurements of the admixture of modes leaving its end. Light guided along unclad fibers was considerably less distorted than light propagating along similar clad waveguides.

I. INTRODUCTION

The possibility of using glass fibers as dielectric waveguides in optical communication systems is well known. This paper describes the light ($\lambda = 6328$ Å) transmission properties of unclad glass fibers surrounded by index matching oil. Their characteristics are compared with those of similar clad fibers in which the cladding was glass. Two types of optical measurements were made: the attenuation and the state of polarization of the light from a fiber end.

Measurements were made on several sizes of fibers (28 μm and 13 μm diameter unclad fibers; 19 μm and 3 μm core diameter clad fibers).* The index of refraction of the oil medium surrounding unclad fibers was varied to mismatch the bulk glass by 8.94, 3.05, and 1.17 percent. The clad fibers were surrounded by glass whose refractive index was 0.824 percent lower than that of the bulk material.[1]

---

* All fibers were manufactured by DeBell and Richardson, Inc. of Hazardville, Connecticut. The bulk material of the core was SSK1 glass. Its index of refraction was measured to be 1.614 at 6328 Å.

II. EXPERIMENTAL APPARATUS AND PROCEDURE

Figure 1 illustrates the laboratory set-up used to make measurements on fibers immersed in oil. The input end of the fiber was rigidly clamped relative to the laser beam, while the output end was immersed in oil to reduce light reflections. Power output was measured with a solar cell which was loaded with a 1000 Ω impedance to ensure detector linearity. The output light power was maximized by adjusting the position of the fiber's input end with a three-dimensional micromanipulator.

Several problems arose when unclad fibers were immersed in oil. Since they are not coated, unclad fibers are sensitive to surface contamination. They were cleaned with methyl ethyl ketone and then threaded through twin iris supports. A black cardboard holding the supported fiber was then placed on top of the oil trough. The input end of the fiber was clamped rigidly and fastened to the window of the oil trough. By sliding the cardboard away from the window the supported fiber could be lowered into the trough without touching its walls. Light was focused into the fiber while it was still suspended in air so that the input tip could be easily located once it was immersed

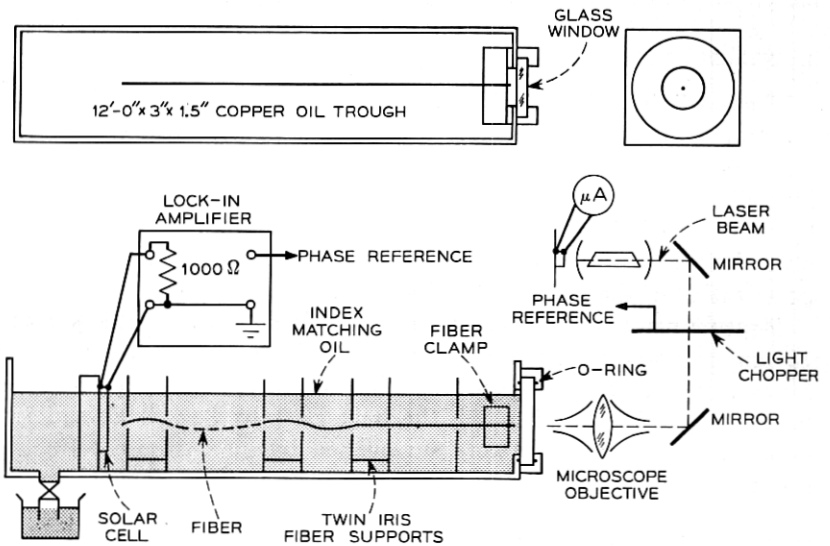

Fig. 1—Experimental arrangement for transmission measurements on fibers immersed in oil.

in index matching oil. Irised supports were employed to ensure that the light scattered from the fiber was a negligible portion of the detected light intensity. Light from the end of a fiber did not vary substantially in power as a function of the number of supports.

The refractive index of the bulk material and oil samples was measured with an Abbe refractometer. However, the refractive index of fibrous glass is in some doubt. The following procedure, illustrated in Fig. 2, was used to make a direct measurement. Laser light was focused into a 28 μm unclad fiber whose input and output tips were suspended in air. A small section of fiber was immersed in oil and its output observed. Energy transmitted through the fiber appeared to be cutoff when the refractive index of the oil cladding was adjusted to be $\Delta = 0.614$ percent less than the index of the bulk glass (i.e., $n_D = 1.6041$ at 6328 Å). This apparent deviation from the bulk glass property may have been caused by the quenching of the glass imposed by the fiber drawing process.[2]

The character of the fiber's output was analyzed by using a $\lambda/4$ plate in conjunction with a polaroid analyzer (refer to Fig. 3a and b) to measure the Stokes parameters[3] (S_T , S_1 , S_2 , S_3) of the light. Define I_1 , I_2 , I_3 , I_4 to be the light powers transmitted through a polaroid sheet when it is oriented parallel to the vectors $\mathbf{e}_1$, $\mathbf{e}_2$, $\mathbf{e}_3$, and $\mathbf{e}_4$ as shown in Fig. 4. I_5 and I_6 are transmitted powers when the polaroid follows a $\lambda/4$ plate which produces a phase difference of $\pi/2$ between $\mathbf{e}_1$ and $\mathbf{e}_2$.

Four measurements are necessary to determine S_T , S_1 , S_2 , S_3 :

(*i*) The total power of the beam, S_T , without the polaroid.
(*ii*) The degree of plane polarization with respect to two arbitrary orthogonal axes, $S_1 = I_1 - I_2$.
(*iii*) The degree of plane polarization with respect to a set of orthogonal axes oriented at 45° relative to the previous set, $S_2 = I_3 - I_4$.
(*iv*) The degree of circular polarization, $S_3 = I_5 - I_6$.

Partially polarized light may be split into two parts: one of power

$$S_p = (\sqrt{S_1^2 + S_2^2 + S_3^2})^{\frac{1}{2}} \tag{1}$$

which is polarized and the other of power $S_T - S_p$ which is unpolarized. The polarized fraction of light, p, can be computed from:

$$p = \frac{S_p}{S_T}. \tag{2}$$

The character of the polarized fraction of light may be expressed in

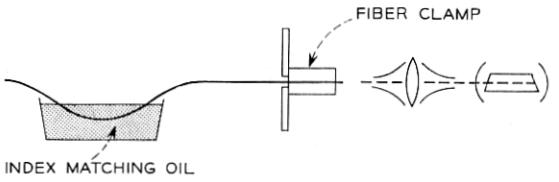

Fig. 2—Arrangement used to determine the refractive index of the unclad fiber core.

terms of the monochromatic electric field strength, **E**, relative to the orthogonal axes $\mathbf{e}_1$ and $\mathbf{e}_2$:

$$\mathbf{E} = b_1 \exp [i(\omega t + \delta_1)]\left\{\mathbf{e}_1 + \frac{b_2}{b_1} \exp [-i(\delta_1 - \delta_2)]\mathbf{e}_2\right\}. \quad (3)$$

Equation (3) may be simplified by defining the complex polarization factor, $\bar{Q} = b_2/b_1 \exp [-i(\delta_1 - \delta_2)]$, which uniquely describes the

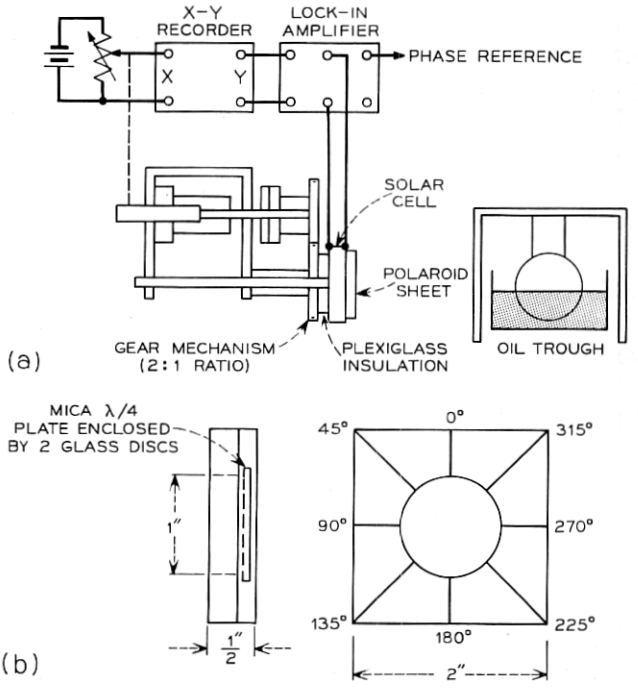

Fig. 3—Schematics of: (a) polaroid analyser and (b) λ/4 plate.

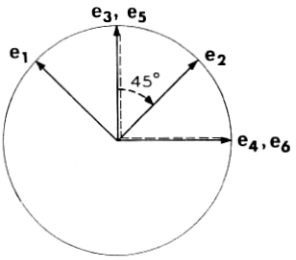

Fig. 4—Polaroid sheet orientations for Stokes parameter measurements. The direction defined by $\mathbf{e}_3$ corresponded to the optic axis of the polaroid when the sheet was adjusted for maximum transmission of linearly polarized laser light. The set of orthogonal axes defined by $\mathbf{e}_1$ and $\mathbf{e}_2$ are oriented at 45° counterclockwise from $\mathbf{e}_3$ and $\mathbf{e}_4$. Axes $\mathbf{e}_5$ and $\mathbf{e}_6$ correspond to measurements made when the polaroid follows a $\lambda/4$ plate which produces a phase difference of $\pi/2$ between directions $\mathbf{e}_1$ and $\mathbf{e}_2$.

polarization of an electromagnetic wave.

$$\mathbf{E} = b_1 \exp\,[i(\omega t + \delta_1)]\{\mathbf{e}_1 + \bar{Q}\mathbf{e}_2\}. \tag{4}$$

The magnitude and phase of $\bar{Q}$ may be expressed in terms of the Stokes parameters:[4]

$$\bar{Q} = \left[\frac{1 - \dfrac{S_1}{S_p}}{1 + \dfrac{S_1}{S_p}}\right]^{\frac{1}{2}} \exp\,(-i\tan^{-1})\left(-\frac{S_3}{S_2}\right). \tag{5}$$

To make a polarization measurement, a polaroid sheet was rotated in the light to be analysed. The polaroid was mounted on the geared mechanism in Fig. 3a which was used to drive a precision potentiometer. The angular position of the polaroid sheet was recorded on the x-axis of an $x - y$ recorder. The light power transmitted through the polaroid was collected by a solar cell and drove the y-axis of the recorder.

By convention, the direction defined by $\mathbf{e}_3$ in Fig. 4 corresponded to the optic axis of the polaroid when the sheet was adjusted for maximum light transmission. Curve (*i*) on Fig. 5, made in linearly polarized laser light, is a profile of the transmitted light power, I, as a function of the angle, θ, measured clockwise between $\mathbf{e}_3$ and the polaroid's optic axis.

Curve (*ii*) in Fig. 5 was obtained when the polaroid followed a $\lambda/4$ plate which produced a phase difference of $\pi/2$ between $\mathbf{e}_1$ and $\mathbf{e}_2$ of Fig.

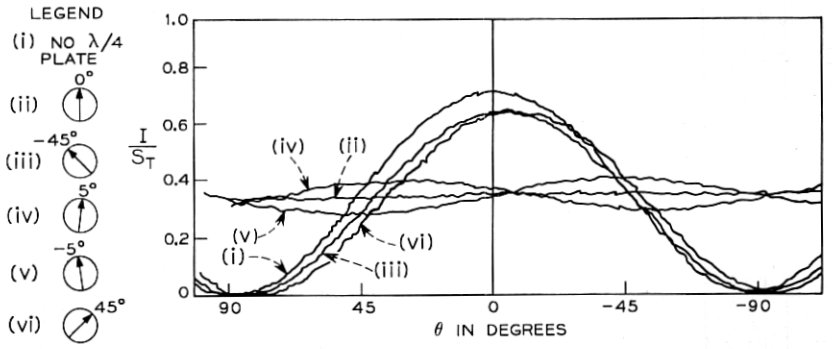

Fig. 5—Polarization calibration in linearly polarized laser light. The normalized light power, I/S_T, was measured as a function of θ, the clockwise angle between the polaroid's optic axis and the vertical reference direction, $\mathbf{e}_3$. A reference axis on the $\lambda/4$ plate was aligned with the direction defined by $\mathbf{e}_3$ when the plate was adjusted to produce a phase difference of $\pi/2$ between $\mathbf{e}_1$ and $\mathbf{e}_2$. Curves *ii–vi* correspond to 5 different orientations of the plate's reference axis relative to $\mathbf{e}_3$.

4. The linearly polarized light which was incident on the plate became circularly polarized and the amount of light transmitted by the polaroid sheet was the same for all orientations. The remaining curves of Fig. 5 correspond to four additional $\lambda/4$ plate orientations relative to $\mathbf{e}_3$. They are each consistent with a different alignment of Fig. 4. For example, the figure would have to be rotated 45° counterclockwise in order to serve as a reference for the $\lambda/4$ plate orientation corresponding to curve (*iii*). The polarized power of the light, S_p, should be invariant to rotation of Fig. 4. The quality of the $\lambda/4$ plate was assessed by comparing S_p computed for the five orientations: (*ii*) through (*vi*). The maximum deviation arose between (*ii*) and (*vi*) and only amounted to 1.82 percent.

Several correcting factors had to be determined before the Stokes parameters could be measured absolutely. Two different solar cells were employed. One detector was used to measure light transmitted through the polaroid (i.e., S_1, S_2, S_3). The other was used to measure the total power, S_T. The sensitivity and linearity of both detectors were compared in the same beam. The transmissivity, $T_{r_{pol.}} = I_3/S_T = 0.748$, of the polaroid sheet in oil was measured by comparing the light power transmitted when its optic axis was parallel to $\mathbf{e}_3$ with the total power. The transmissivity of the $\lambda/4$ plate in oil, $T_{r_{\lambda/4}} = I/S_T = 0.947$, was measured by comparing the light power transmitted through it with the total power.

Figure 6 illustrates typical measurements of the state of polarization

of the partially polarized light leaving sample fiber lengths. Curve (a) in Fig. 6 offers consecutive measurements for three different end cuts of the same 19 μm clad fiber which had been totally immersed in oil. It illustrates that end effects are negligible for immersed fibers.

Two profiles, of I versus θ, appear for each measurement in Fig. 6. One profile was obtained when the polaroid followed a $\lambda/4$ plate which produced a phase difference of $\pi/2$ between $\mathbf{e}_1$ and $\mathbf{e}_2$. It was used to determine S_3 . The other profile was obtained without the $\lambda/4$ plate and was used to determine S_1 and S_2 . The three parameters S_1 , S_2 , and S_3 were normalized relative to the total power, S_T , and were used to compute the polarized fraction of light, p, from equations (1) and (2) along with the complex polarization factor, $\bar{Q}$, from equation (5). Comparison of Figs. 6a and 6c with Fig. 6b illustrates that the degree of circular polarization, determined from the measurement with

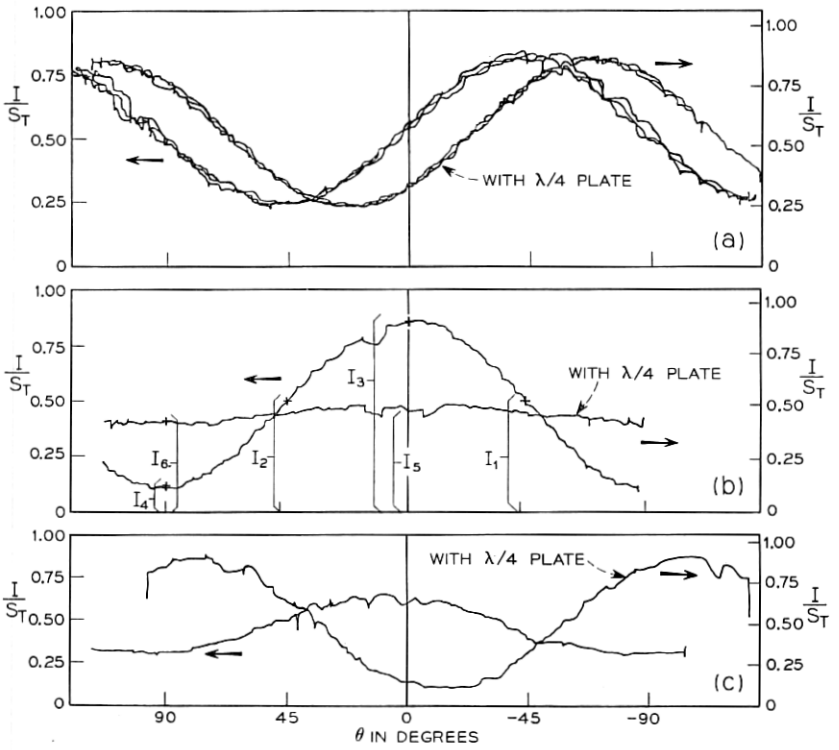

Fig. 6—Sample profiles of I/S_T vs θ for partially polarized light leaving: (a) 19μm clad fiber (L = 301 cm, Δ = 0.824%), (b) 28μm unclad fiber (L = 238 cm, Δ = 2.44%), and (c) 28μm unclad fiber (L = 197 cm, Δ = 0.56%).

the $\lambda/4$ plate, could vary over a wide range. The analysis based on the profiles in Fig. 6b are included in that figure. The analysed light was 75 percent polarized. Its polarized fraction was characterized by $\bar{Q} = 1.04 \exp(i2.9°)$. Such results should be independent of light power and they were approximately so. Figure 7a is a plot of p versus normalized input power for a 31-cm length of 28 μm fiber with $\Delta = 2.44$ percent. Figure 7b shows $\bar{Q}$ plotted in the complex plane with light intensity as the parameter. The points are numbered sequentially to correspond to points of Fig. 7a reading from right to left. If depolarization had not occurred the light would have been 100 percent polarized (i.e., $p \equiv 1$) and all data points in the complex $\bar{Q}$ plane would have been located at $1 \mid 0°$. The results of Fig. 7a and b indicates that p, arg. $\bar{Q}$, $\mid \bar{Q} \mid$ deviated by only ± 3.7 percent, $\pm 2.5°$, ± 13 percent from their mean values when the input power was doubled.

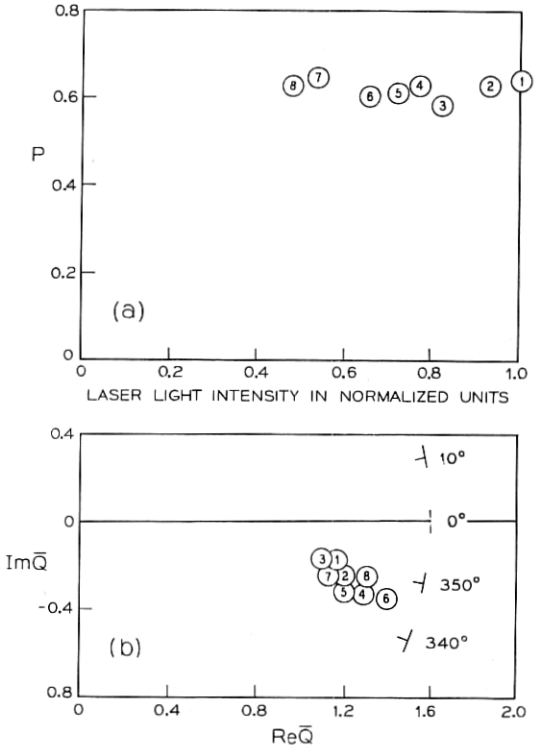

Fig. 7—The state of polarization of a 28μm unclad fiber ($L = 30$ cm, $\Delta = 2.44\%$) analysed as a function of input power: (a) p vs normalized laser light power, (b) $\bar{Q}$ is plotted in the complex plane with light power as the parameter. The points are numbered sequentially to correspond to the points of (a) reading from right to left.

III. MEASUREMENTS ON FIBERS

Optical properties of fibers were measured as a function of fiber length, L, measured from the input tip. The length was changed by cutting off known decrements of fiber. Some figures contain several sets of data points. Each set of points corresponded to a different fiber. Although laser power was not kept constant between runs, it remained stable during the course of a single set of measurements.

The transmission loss coefficient, α, of a fiber is determined from the slope of a semi-logarithmic plot of detector output, I, versus L.

Since:

$$I = I_0 \exp(-\alpha L) \tag{6}$$

then

$$\alpha = -\frac{\ln \frac{I}{I_0}}{L}. \tag{7}$$

Figure 8a and b illustrate transmission measurements made on two different 13 μm unclad fibers which had been immersed in oil whose refractive index was 2.44 percent lower than the index of the fibrous core at 6328 Å. The data points, labeled sequentially reading from right to left, are coded to correspond to polarization measurements made on the same fibers and recorded in Fig. 9. Light power, I, was measured in terms of the scale units of a lock-in amplifier. The attenuation coefficient of unclad fibers increased markedly and the power input, I, deviated from an exponential dependence on L for $L < 1m$. This behavior was probably related to launching phenomena. It was inconsequential since measurements were always made on lengths long enough to make transmission properties solely dependent upon fiber parameters. Occasionally, lack of linearity was noted near the ends of unclad fiber. These apparent increases in attenuation occurred along lengths of fiber which had become contaminated upon contact with a dusty surface. Figure 8c illustrates transmission measurements made on a 3 μm clad fiber. The data points are coded to correspond to polarization measurements recorded in Fig. 10. The discontinuity at data point 7 of Fig. 8c was due to a gross imperfection within the core or at the core cladding interface of the 3 μm clad fiber.

Transmission measurement results, for clad and unclad fibers, are summarized in Table I. The loss measurements made on clad fibers served to calibrate the experimental technique. They are consistent

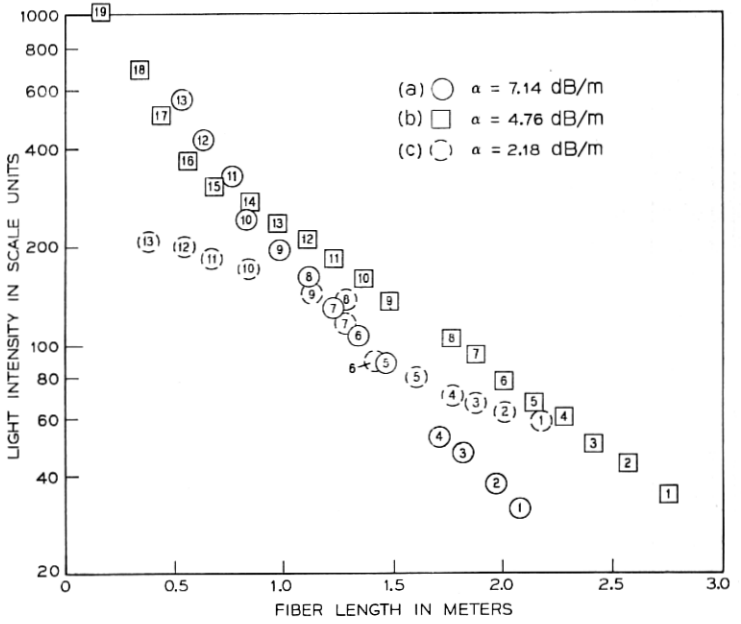

Fig. 8—(a, b) Transmission loss measurements along two different 13 μm unclad fibers immersed in oil ($\Delta = 2.44\%$). (c) Transmission loss measurements along a 3μm clad fiber.

with results originally obtained by A. R. Tynes, et al.[1] Fiber diameter (2a), the index mismatch between the core and its surroundings (Δ), the asymptotic value of the polarized fraction of light for long lengths of fiber (p_0), the characteristic number of the fiber waveguide

$$\left(R = \frac{2\pi a}{\lambda}(n_1(n_1^2 - n_2^2))^{\frac{1}{2}} \simeq (2.8)\frac{\pi a}{\lambda} n_1^{\frac{3}{2}} \Delta^{\frac{1}{2}}\right),$$

and the approximate number of propagating modes (N) appear as parameters. Loss coefficients of the oil media surrounding the immersed fibers were measured on an optical loss-gain measuring set.[5] Those results, included in Table II, and the analysis outlined in Appendix B indicate that the fraction of α due to energy propagating within the oil was less than 3 percent.

The data listed in Table I indicates that the attention constant, α, increases for decreasing fiber diameter, 2a, and index mismatch, Δ, but remains approximately constant when the preceding parameters

are changed in a manner which keeps the number of modes constant. In general, unclad fibers were much more lossy than similar glass fiber waveguides. Unavoidable surface contamination of the exposed surfaces may explain this deviation.

The guiding quality of a fiber may be estimated by measuring the state of polarization of light leaving its end. Linearly polarized light having a Gaussian distribution was launched into a series of multi-mode fibers. The minimum number of propagating modes was seven for clad fiber and 210 for unclad fiber. The input light conformed to the dominant mode of each of the fibers tested. At best, for fibers free of irregularities in geometry and refractive index all propagating energy would remain in the dominant mode and $p \equiv 1 \equiv \bar{Q} \equiv 1$. For poor guiding structures the energy originally in the dominant mode should eventually become

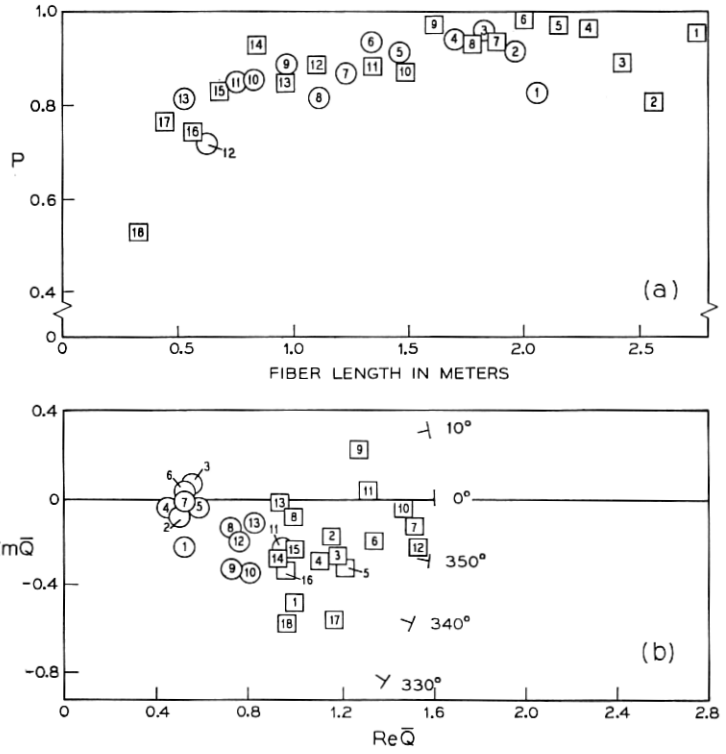

Fig. 9—Analyses of the states of polarization along two different 13μm unclad fibers ($\Delta = 2.44\%$): (a) p vs fiber length, and (b) $\bar{Q}$ is plotted in the complex plane with fiber length as the parameter. The points are numbered sequentially to correspond to the points of (a) and Figure 8a, b reading from right to left.

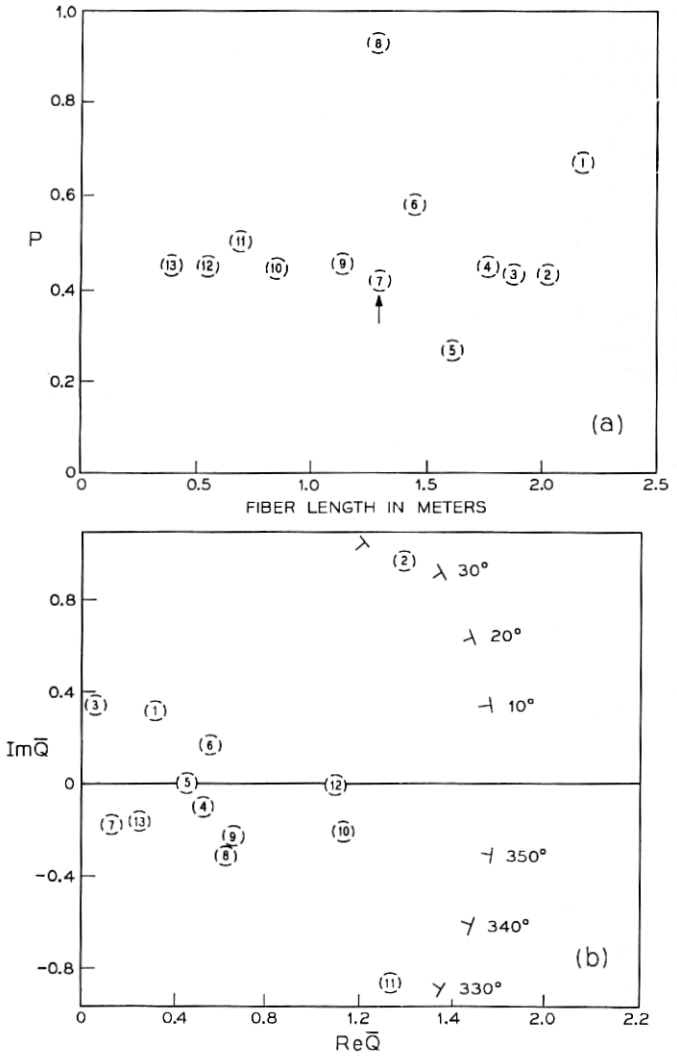

Fig. 10—Analyses of the states of polarization along a 3μm clad fiber ($\Delta = 0.824\%$): (a) p vs fiber length. The notation ↑ refers to a bright spot indicative of a gross defect within the core or at the core cladding interface. (b) $\bar{Q}$ is plotted in the complex plane with fiber length as the parameter. The points are numbered sequentially to correspond to the points of (a) and Figure 8c reading from right to left.

distributed among all possible propagating modes. The state of polarization for this case is analysed[6] in Appendix B assuming equal power in all modes. The analysis indicates that the fraction of polarized light, $p \to 1/2$ as the number of modes, $N \to \infty$ (i.e., $\lim_{N\to\infty} p = 1/2$).

The laser light launched into all fibers was linearly polarized and consequently the ratio between the polarized and total powers was $p = 1$. Some depolarization was observed in both clad and unclad fibers for measured lengths as small as 5 cm. In unclad fibers, the fraction of polarized light appeared to increase towards an asymptotic value, $p_0 = 1$, for increasing fiber length. The length at which light became completely polarized depended upon the total number of propagating modes. Figure 9a shows sample plots of p versus fiber length for two different 13 μm unclad fibers with $\Delta = 2.44$ percent. Transmission measurements for these fibers are included in Fig. 8a and b. Figure 9b illustrates corresponding plots of $\bar{Q}$. Points in the complex plane are numbered sequentially to correspond to the data points of 9a, reading from right to left. The fact that the imaginary component of $\bar{Q}$ was not negligible for many of the data points in Fig. 9b indicates that the polarized fraction of light, propagating within fibers, can contain significant elliptically polarized components. This type of depolarization may have been due to small guide imperfections which caused the power in the fundamental mode to become distributed among other propagating modes. The phase of a wave can be significantly distorted after propagating short distances when the phase velocity difference between modes is small, as for the slightly elliptical cross-section considered in Appendix C. Ellipticities like that could have been caused by squeezing during the fiber drawing process.

Figure 10 was laid out in the same format as Fig. 9. Corresponding transmission results are included in Fig. 8c. They apply to measurements made on a 3 μm clad fiber which had been immersed in oil to

TABLE I—SUMMARY OF OPTICAL MEASUREMENTS

	Unclad Fibers					Clad Fibers	
2a(μm)	28			13		19	3
Δ (%)	8.32	2.44	0.56	8.32	2.44	0.824	0.824
α (db/m)	2.39	3.92	4.58	3.83	5.71	1.83	2.18
p_0	not measured	1.0	1.0	not measured	1.0	0.50	0.50
R	116	62	29	53	29	25	4
N	>800	800	200	700	200	160	7

TABLE II—TRANSMISSION LOSS IN INDEX MATCHING OILS

Δ (%)	8.32	2.44	0.56
α^* (db/m)	1.85	4.96	4.14

* The transmission loss coefficient, α, of the bulk glass from which all fibers were drawn was measured to be 1.46 dB/m.[1]

eliminate end effects. Light scattering from the cladding was eliminated by matching the oil to the glass cladding. Considerably more unpolarized light propagated along clad fibers than along similar unclad fibers. In addition, the repeatability of results, for clad fibers was not nearly as good and the measurement fluctuations could be much worse than for unclad fibers. Some of these fluctuations resulted from gross imperfections within the core or at the core cladding interface. One such defect is apparent within the 3 μm clad fiber in the vicinity of data point 7.

The 3 μm clad fiber was considerably less multimode than any of the other fibers tested. Its characteristic number was $R = 3.93$ and it could only support seven modes. For some reason, however, the clad fiber was more of a depolarizer since $p \to p_0$ for lengths as small as $L = 0.4$ m. This was considerably smaller than the corresponding length, $L = 1.5$ m, for unclad fibers with $R = 29$, but was consistent with the decrease in the number of propagating modes.

The asymptotic limit, p_0, of the polarized fraction of light propagating within clad and unclad fibers has been tabulated in Table I. The results imply that unclad fibers are relatively good guiding structures. Clad fibers, by contrast, are extremely poor waveguides since linearly polarized light quickly becomes distributed equally among all possible propagating modes.

IV. CONCLUSIONS

Electromagnetic energy was more highly attenuated within unclad fibers immersed in oil than within glass clad waveguides capable of supporting the same number of modes. The attenuation constant, α, increased for decreasing fiber diameter, 2a, and index mismatch, Δ. However, α remained approximately constant when the preceding parameters were changed in a manner which kept the number of modes constant (i.e., the characteristic number $R \simeq (2.8)(\pi a/\lambda)n_1^{\frac{3}{2}}\,\Delta^{\frac{1}{2}} =$ constant). For the unclad fibers α varied from a high of 4.58 dB/m for a guide characterized by $R = 29$ to a low of 2.39 dB/m when $R = 116$.

For clad fibers α varied from a high of 2.18 dB/m when $R = 3.93$ to a low of 1.83 dB/m when $R = 25$.

Light leaving the end of a fiber may be divided into three components: unpolarized, linearly polarized, and circularly polarized light. The guiding quality of a multimode fiber waveguide, excited by completely linearly polarized laser light, was estimated by measuring the ratio, p, between the polarized and unpolarized light powers leaving its end. At best, $p = 1$ if the guided energy is not coupled to any unpolarized modes. For poor guiding structures, $p = 1/2$ if the guided energy becomes distributed equally among all propagating modes. Based on this criteria unclad fibers appear to be much better ($p \rightarrow 1$) guiding structures than clad fibers ($p \rightarrow 1/2$). This behavior in guiding quality is consistent with the attenuation measurements which indicate that glass clad fibers, with their lower loss coefficients, can contain more light modes than oil clad fibers can.

The polarized fraction of light leaving some fibers had significant circularly polarized components which could have been due to a slight cross-sectional ellipticity caused by squeezing during the fiber drawing process.

V. ACKNOWLEDGMENT

The author gratefully acknowledges the many helpful suggestions of E. A. J. Marcatili and A. R. Tynes.

APPENDIX A

Loss Coefficient Error Due to Energy Propagating Outside the Fiber Core

In a dielectric waveguide all but the TE_{0m} and TM_{0m} modes are hybrid. Both **E** and **H** have nonzero components along the axis of the guide. If E_z makes the dominant contribution to a transverse component of E, then the mode is designated as EH_{nm}. If H_z makes the dominant contribution, then the mode is designated as HE_{nm}.

The number and kind of modes which may propagate in a particular waveguide can be identified if the parameter,

$$R = (2\pi a/\lambda)\sqrt{[n_1(n_1^2 - n_2^2)]^{\frac{1}{2}}},$$

is known. This parameter is an upper bound on the zero of the Bessel function[7] corresponding to the highest-order propagating mode. Table I lists transmission results as a function of waveguide parameters. The

minimum value of R, for an unclad fiber, was $R = 29$. By computing the fractional amount of power propagating outside the fiber core for $R = 29$, an upper bound may be determined for the loss coefficient error.

A total of 18 circularly symmetric modes can propagate (i.e., $TE_{01} \rightarrow TE_{09}$ plus $TM_{01} \rightarrow TM_{09}$). An additional 191 hybrid modes may also propagate (the highest order hybrid modes are the $EH_{23,1}$ and $HE_{25,1}$ modes. They are practically degenerate). The fractional amount of power propagating outside the core, I_{ext}/I_{total}, may be estimated by assuming that power is distributed equally among all the modes and that all external power is carried by the doubly degenerate highest order mode:

$$\frac{I_{ext}}{I_{total}} < 1 - \frac{207}{209} = 0.01. \tag{8}$$

The loss coefficients of the core and the external medium both contribute to the transmission loss coefficient, α:

$$\begin{aligned} \alpha &= \frac{I_{core}}{I_{total}} \alpha_{core} + \frac{I_{ext}}{I_{total}} \alpha_{ext} \\ &\approx \alpha_{core}\left(0.99 + 0.01 \frac{\alpha_{ext}}{\alpha_{core}}\right). \end{aligned} \tag{9}$$

The values of α_{ext} for the oil media in which unclad fibers were immersed are listed in Table II.

$$\left(\frac{\alpha_{ext}}{\alpha_{core}}\right)_{max} = \frac{(\alpha_{ext})_{max}}{\alpha_{bulk}} = 3.4. \tag{10}$$

The loss coefficient error, e, may be estimated after substituting equation (10) into equation (9).

$$e = \frac{\alpha - \alpha_{core}}{\alpha_{core}} \times 100 = 2.4\%. \tag{11}$$

APPENDIX B

Derivation of the State of Polarization of Light in Terms of Its Mode Content

Consider a square fiber of side, a, which can support N^2 modes. In Section II and Fig. 4 the Stokes parameters (S_T, S_1, S_2, S_3) were defined in terms of power transmitted through a polaroid sheet. The Stokes parameters of guided light leaving the end of a square fiber

will now be expressed in terms of the electric field components of each mode in the transverse plane of the guide.

$$S_T = \int_{-a/2}^{a/2}\int_{-a/2}^{a/2} \{|E_x|^2 + |E_y|^2\}\, dx\, dy, \tag{12}$$

$$S_1 = I_1 - I_2 = \int_{-a/2}^{a/2} \left\{ \left| \frac{1}{\sqrt{2}}(E_y - E_x) \right|^2 - \left| \frac{1}{\sqrt{2}}(E_y + E_x) \right|^2 \right\} dx\, dy,$$

$$S_1 = \int_{-a/2}^{a/2}\int_{-a/2}^{a/2} -2\,|E_y E_x|\, dx\, dy, \tag{13}$$

$$S_2 = I_3 - I_4 = \int_{-a/2}^{a/2}\int_{-a/2}^{a/2} \{|E_y|^2 - |E_x|^2\}\, dx\, dy. \tag{14}$$

The polarized fraction of each mode is linearly polarized since there is no phase shift between its x and y field components. Therefore:

$$S_3 = I_5 - I_6 = 0. \tag{15}$$

The polarized fraction of light, p, can be computed from:

$$p = \frac{[S_1^2 + S_2^2 + S_3^2]^{\frac{1}{2}}}{S_T} = \frac{\left[\left(\int_{-a/2}^{a/2}\int_{-a/2}^{a/2} -2\,|E_y E_x|\, dx\, dy\right)^2 + \left(\int_{-a/2}^{a/2}\int_{-a/2}^{a/2} \{|E_y|^2 - |E_x|^2\}\, dx\, dy\right)^2\right]^{\frac{1}{2}}}{\int_{-a/2}^{a/2}\int_{-a/2}^{a/2} \{|E_x|^2 + |E_y|^2\}\, dx\, dy} \tag{16}$$

For small differences in indices of refraction between the core and its cladding and for modes far from cut-off, the transverse field in a dielectric guide closely resembles the field in a similar metallic waveguide. The transverse electric field components corresponding to modes in a square metallic waveguide are:[9]

TM_{mn} modes:

$$\left.\begin{aligned} E_{x_{mn}} &= \frac{-j}{\left[1 - \left(\frac{k_{c_{mn}}}{k}\right)^2\right]^{\frac{1}{2}}} \frac{k_n k}{k_{c_{mn}}^2} A \sin k_m x \cos k_n y \\ E_{y_{mn}} &= \frac{j}{\left[1 - \left(\frac{k_{c_{mn}}}{k}\right)^2\right]^{\frac{1}{2}}} \frac{k_m k}{k_{c_{mn}}^2} A \cos k_m x \sin k_n y \end{aligned}\right\} \exp(-ik_{z_{mn}} z + i\omega t), \tag{17}$$

TE_{mn} modes:

$$\left.\begin{aligned} E_{x_{mn}} &= j\sqrt{\frac{\mu}{\epsilon}}\,\frac{k_n k}{k_{c_{mn}}^2}\,B\cos k_m x \sin k_n y \\ E_{y_{mn}} &= -j\sqrt{\frac{\mu}{\epsilon}}\,\frac{k_m k}{k_{c_{mn}}^2}\,B\sin k_m x \cos k_n y \end{aligned}\right\} \exp\,(-ik_{z_{mn}}z + i\omega t) \tag{18}$$

where:

$$\begin{aligned} k_m^2 + k_n^2 + k_{z_{mn}}^2 &= n_1^2 k^2, \\ k_m = \frac{m\pi}{a}, \qquad k_n &= \frac{n\pi}{a}, \qquad k_{c_{mn}} = (k_m^2 + k_n^2)^{\frac{1}{2}}. \end{aligned} \tag{19}$$

The following results apply to both TE and TM modes.

By using the orthogonality property of sines and consines one can show that:

$$\int_{-a/2}^{a/2}\int_{-a/2}^{a/2} |\, E_{x_{mn}} E_{y_{mn}} \,|\, dy = 0, \tag{20}$$

$$\int_{-a/2}^{a/2}\int_{-a/2}^{a/2} |\, E_{x_{mn}} \,|^2\, dx\, dy \propto \left(\frac{a}{2}\right)^2, \tag{21}$$

$$\int_{-a/2}^{a/2}\int_{-a/2}^{a/2} |\, E_{y_{mn}} \,|^2\, dx\, dy \propto \left(\frac{a}{2}\right)^2. \tag{22}$$

Substitute equations (20), (21) and (22) into equation (16):

$$p_{mn} = \left|\frac{k_m^2 - k_n^2}{k_m^2 + k_n^2}\right| = \left|\frac{m^2 - n^2}{m^2 + n^2}\right| \tag{23}$$

where: $0 \leqq m \leqq N$, $0 \leqq n \leqq N$ but $m = n \neq 0$.

Equation (23) is an expression for the polarized fraction of any mode within a square metallic waveguide. It is approximately correct for square dielectric guides if $\Delta \ll 1$ and if the mode is far from cut-off.

As an example assume that the total power within the guide is distributed equally among all propagating modes. Equation (23) may be used to compute p by averaging p_{mn} over all propagating modes.

$$p = \frac{1}{N^2}\sum_{\substack{m=0,n=0\\ m=n\neq 0}}^{m=N,n=N} p_{mn} \approx \frac{1}{N^2}\int_{m=0}^{N}\int_{m=0}^{N}\left|\frac{m^2 - n^2}{m^2 + n^2}\right| dm\, dn. \tag{24}$$

The integration may be simplified after referral to Fig. 11 which illustrates values of p_{mn} projected onto the $m - n$ plane. p_{mn} is constant along radial lines passing through the origin at $m = n = 0$. In the limit $N \to \infty$ the integral over the $N \times N$ square may be replaced

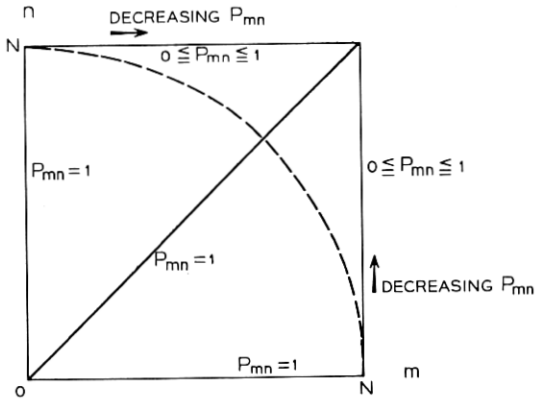

Fig. 11—Values of p_{mn} are shown projected onto the $m - n$ plane. If $N \to \infty$ then the $N \times N$ square domain of definition for p_{mn} may be replaced by the dashed circle of radius N.

by an integral over a circle of radius N and centered at the origin. Define:

$$m = R \cos \Phi, \qquad n = R \sin \Phi, \tag{25}$$

$$p \approx \frac{2}{N^2} \int_{\Phi=0}^{\pi/4} \int_{R=0}^{N} p_{mn} R \, dR \, d\Phi. \tag{26}$$

Now substitute equation (25) into equation (26)

$$\lim_{N\to\infty} p = \frac{2}{N^2} \int_{\Phi=0}^{\pi/4} \int_{R=0}^{N} (\cos^2 \Phi - \sin^2 \Phi) R \, dR \, d\Phi = \tfrac{1}{2}. \tag{27}$$

APPENDIX C

Circular Polarization Induced in a Slightly Elliptical Fiber

Consider a fiber of elliptical cross section having major and minor axes a, b. Two fundamental modes polarized along a and b have a phase shift $(k_z - k_z')L$ after propagating a distance, L.

To calculate $(k_z - k_z')$ we roughly approximate the fiber's elliptical cross-section by a rectangle of sides a and b. From Ref. 8 we get the axial propagation constant of the dominant mode polarized along a:

$$k_z = \frac{2\pi}{\lambda} n_1 \left[1 - \left(\frac{\lambda}{2an_1} \right)^2 \left(1 + \frac{2A}{\pi a} \right)^{-2} \right]^{\frac{1}{2}} \tag{28}$$

where:

$$A = \frac{1}{2^{\frac{1}{2}} n_1} \frac{1}{\sqrt{\Delta}}.$$

In multi-mode guides:

$$\frac{2A}{\pi a} \ll 1 \tag{29}$$

and

$$k_z \approx \frac{2\pi}{\lambda} n_1 \left\{1 - \left(\frac{\lambda}{2an_1}\right)^2 \frac{1}{2}\left(1 - \frac{4A}{\pi a}\right)\right\}. \tag{30}$$

Thus:

$$(k_z - k_z')L \approx \frac{\pi\lambda}{4n_1} L\left\{\left(\frac{1}{b^2} - \frac{1}{a^2}\right) + \frac{4A}{\pi a^2}\left(\frac{1}{a} - \frac{a^2}{b^2}\frac{1}{b}\right)\right\}. \tag{31}$$

Assume:

$$\frac{b-a}{a} \ll 1, \qquad \frac{1}{b} = \frac{1}{a + (b-a)} \approx \frac{1}{a}\left\{1 - \frac{b-a}{a}\right\}. \tag{32}$$

Then:

$$(k_z - k_z')L \approx \frac{\pi}{2n_1}\frac{\lambda}{a}\frac{L}{a}\left(\frac{a-b}{a}\right)\left\{1 - \frac{6A}{\pi b}\right\}. \tag{33}$$

Choose as an example:

$$a = 28\mu m, \quad L = 1m, \quad n_1 = 1.604, \quad \left(\frac{a-b}{a}\right) = 0.01, \quad \Delta = 0.0056.$$

The phase shift after one meter is:

$$(k_z - k_z')L = 2.52\pi(1 - 0.127). \tag{34}$$

This phase shift is significant even for the small ellipticity assumed.

REFERENCES

1. Tynes, A. R., Pearson, A. D., and Bisbee, D. L., to be published in J. Opt. Soc., February 1971.
2. Otto, W. H., "Compaction Effects in Glass Fibers," J. Am. Cer. Soc., *44*, No. 2 (February 1961), pp. 68–72.
3. Ditchburn, R. W., *Light*, New York: Interscience Publishers, Inc., 1963, pp. 480–483.
4. Beckmann, P., *The Depolarization of Electromagnetic Waves*, Boulder, Colorado: The Golem Press, 1968, pp. 24–35.
5. Tynes A. R., and Bisbee, D. L., unpublished work.
6. Marcatili, E. A. J., unpublished work.
7. Beattie, C. L., "Table of First 700 Zeroes of Bessel Functions," B.S.T.J., *37*, No. 3 (May 1958), pp. 689–697.
8. Marcatili, E. A. J., "Dielectric Rectangular Waveguide and Directional Coupler for Integrated Optics," B.S.T.J., *48*, No. 7 (September 1969), pp. 2071–2102.
9. Ramo S., and Whinnery, J. R., *Fields and Waves in Modern Radio*, New York: Wiley, Inc., 1953, p. 366.